ERASMUS UNIVERSITY ROTTERDAM

ERASMUS UNIVERSITY ROTTERDAM

Erasmus School of Economics

Bachelor Thesis: Econometrics and Operational Research

Three-stage MLR, ANN and MARS models for long-term hourly load forecasting

Student name:	Breukelen, L.W.F. van
Student ID number:	484757
Supervisor:	Vermeulen, S.H.L.C.G.
Second assessor:	Oorschot, J.A.
Date final version:	02/07/2020

Abstract Electric load forecasts are vital to ensure reliable power supply. Load forecasts are especially important, since power storage capacity is small. This paper evaluates the performance of MLR, ANN and MARS models for modelling relationships between the hourly load demand in Luxembourg and seasonal patterns, calendar effects as well as weather and economic variables. ANN and MARS models forecast the hourly load demand more accurately than the MLR model, which performance is especially lower if the relationships between variables seem to be more complex. Incorporating uncertain weather and economic variables in the models does not enhance long-term out-of-sample forecasts, but the developed models are nevertheless useful in other applications.

Contents

1 Introduction 1

2 Literature 3

3 Data 6

4 Methodology 9

4.1 Multiple Linear Regression (MLR) 10

4.2 Artificial Neural Network (ANN) 10

4.3 Multivariate Adaptive Regression Splines (MARS) 12

4.4 Double seasonal block bootstrap 13

5 Explanatory variables 14

6 Results 16

7 Conclusion 20

8 Recommendations 20

9 Appendix 21

9.1 Additional results 21

9.2 Additional methodology 24

10 MATLAB code 28

1 Introduction

Electric load forecasts are vital for a reliably electric power industry. The forecasts are crucial for decision making in the energy sector. For day-to-day operations such as the determination of production scheduling and energy allocation, but also for long-term decisions such as investments in new facilities. In comparison with other industries, accurate forecasting models for electric load are especially important since electrical energy cannot be massively stored using today's technologies, implying that demand and supply should (almost) match at every moment.

Although there is not a golden standard for classifying the range of load forecasts, Hong and Fan (2016) use a classification with a cut-off horizon of two weeks. Forecasts till two weeks are short-term load forecasts (STLF) and forecasts exceeding two weeks are long-term load forecasts (LTLF). In the existing literature, the LTLF frequency is usually low and the constructed models serve a single, very specific forecasting problem. We make a model for LTLF at intervals of an hour instead. The advantage of our model is the applicability to different load forecasting problems such as: investment decisions, operations and maintenance, transmission and distribution planning as well as demand management. Moreover, the incorporation of high frequency explanatory variables could also enhance forecasting performance. Hong, Wilson, and Xie (2013) conclude that the classical approach for LTLF is often limited to the use of load and weather information occurring with monthly or annual frequency. They find that the use of low resolution and infrequent data can lead to inaccurate forecasts. The high frequency approach in this paper, which takes advantage of hourly information, could therefore result in more accurate and defensible forecasts.

In the absence of statistical software packages in the early ages of load forecasting, an engineering approach was developed to manually forecast the future load using charts and tables. The invention of the computer led to an abundance of load forecasting models. Out of the abundance of methods, we use Multiple Linear Regression (MLR), Artificial Neural Network (ANN) and Multivariate Adaptive Regression Splines (MARS) as in Nalcaci, Özmen, and Weber (2019). The well-known MLR and ANN have extensively been used for load forecasting purposes. Nalcaci et al. (2019) find the performance of the relative uncommonly used MARS model competitive with the ANN model for LTLF, which gives us reason to further investigate the performance of the MARS model.

The goal of this paper is to obtain a method suitable for making LTLF for all long-term forecasting horizons up to three years after the forecast construction date. In order to prevent a look-ahead bias, we only incorporate information which was available on the forecast construction date.

Out of existing literature, Hong et al. (2010) conclude that weather variables, past load, calendar events, and seasonal factors have a significant impact on the load demand. Past load is especially informative for STLF, however becomes increasingly inaccurate if the forecasting horizon increases. Due to the increasing inaccuracy for forecasts further away from the day at which the forecasts are constructed, the use of past load is excluded from our models.

The relationships between the remaining explanatory variables and the load demand can either be modelled in a single-stage model or by a sequence of stages. This paper uses a sequence of three stages, since single-stage models can fail to incorporate multiple types of effects on the load demand simultaneously. Zhang and Qi (2005) state that just as traditional statistical models, ANN is for example not able to simultaneously model many different relationships between the explanatory variables and dependent variable well. In the multi-stage models, the division is commonly based on the type of phenomena which is modelled. Magnano and Boland (2007) for instance, start with modelling the relationship between the load demand and the seasonal patterns, after which they investigate the relationship between the season-adjusted load and weather variables. In our sequence of three stages, the first stage removes the effect of seasonal patterns on the load demand. The second stage investigates the relationship between the deseasonalized load and other calendar events due to national holidays and vacation periods. These calendar events are separated from the seasonal pattern, since it allows us to separately focus on the dominant and complex seasonal patterns before incorporating other effects. Finally, the third stage investigates the relationship between the season- as well as calendar-adjusted load and the weather and economic variables. Since weather and economic variables are unknown for long periods ahead and we want to prevent a look-ahead bias, double seasonal block bootstrap helps constructing different input scenarios. The set of input scenarios leads to a set of forecasts. The average of the set of forecasts results in a single time-series of LTLF, which is the final estimate of the three-stage model.

In summary, this paper investigates the performance of the MLR, ANN and MARS models for LTLF in three consecutive stages, to find the best performing combination of these models. Moreover, we investigate if bootstrap constructed uncertain explanatory variables could enhance the out-of-sample forecasts. This leads to the following research question: What combination of MLR, ANN and MARS models provide the most accurate hourly long-term load forecasts, when applying three consecutive stages?

The European Network of Transmission System Operations for Electricity (ENTSO-E) provides the hourly load data from 01/01/2006 until 31/12/17 for the Grand-Duchy of Luxembourg. Methostat provides the hourly weather data representative for Luxembourg. The measure for the state of the economy is the DAX-index, which Yahoo! Finance provides. The data from 01/01/2006 until 31/12/14 is for construction of the three-stage models. These models are evaluated on the test data, which starts at 01/01/2015 and ends at 31/12/17.

We implement the methods and models in MATLAB R2020a, extended with the Optimisation and Deep Learning Toolbox as well as the MARS/ARESlab Toolbox of Jekabsons (2016). The performance of the resulting models indicates that ANN and MARS models outperform the MLR model, especially if the relationship between the explanatory variables and the dependent variable seems to be more complex. In contrast to the MLR model, the ANN and MARS models find useful functional relationships between weather and economic variables and the load demand which is adjusted for seasonal patterns and calendar effects. These relationships can be utilized for applications such as 'what-if' analyses, but are unable to enhance the out-of-sample forecast performance.

2 Literature

Load forecasting models can be divided in two groups (Hong & Fan, 2016). The first group consists of statistical models, which is further divided into: multiple linear regression (MLR) models, autoregressive and moving average models, semi-parametric additive models and exponential smoothing models. According to Hinman and Hickey (2009) and Nalcaci et al. (2019), the regression models are widely used in electric load forecasting. The term 'regression' in MLR refers to statistical process for estimating the relationships among variables and the term 'linear' to the linear equations that are used to solve the parameters, rather than the relationships between the dependent and independent variables (Hong & Fan, 2016). A MLR model distinguishes itself from a single linear regression model, through the use of multiple explanatory variables instead of a single explanatory variable. The advantage of the MLR model is that it is easy to interpret, implement and use. Nalcaci et al. (2019) conclude however that the forecasts of MLR are less accurate in comparison with alternative load forecasting models. A possible explanation is given by Metaxiotis, Kagiannas, Askounis, and Psarras (2003), which state that misspecification of the functional relationship between the dependent and explanatory variables often is the cause of bad performance.

The second group of load forecasting models consists of artificial intelligence (AI) based models. AI is a relatively new research field, where common load forecasting methods include neural networks, fuzzy regression models, support vector machines and gradient boosting machines. Rosenblatt (1962) describes the usefulness of neural networks for many applications such as model classification and learning methods. Neural networks are generally used for complex data structure applications such as high-dimensional input data applications. By learning patterns from the historical data, without requiring the forecaster to describe a functional relation between the input (explanatory) and output (dependent) variables, a mapping between input and output is constructed. AI models are better in dealing with non-linearity and other difficulties than statistical models, since they do not require any complex mathematical formulation or quantitative correlation between inputs and outputs (Metaxiotis et al., 2003). A disadvantage of AI methods is however that the resulting mapping between input and output lacks the possibility of interpretation, which is reason for Çevik et al. (2017) to see the behaviour of ANN as a 'black box' model.

Many types of neural networks are used for load forecasting, such as feed-forward neural networks, radial basis function networks, and recurrent neural networks. An ANN is a feed-forward neural network based on the biological brain, in which different layers of nodes (neurons) are connected by a network of weights (synapses). The weights and input variables, determine the output or estimate of the model. To improve the forecasts accuracy, the weights are adjusted through an iterative supervised training process. Rumelhart, Hinton, and Williams (1986) use backpropagation to train a neural network. Hagan and Menhaj (1994) incorporate the Levenberg-Marquardt algorithm (Marquardt, 1963) into the backpropagation algorithm for training feed-forward neural networks and obtain more efficient results for small neural networks, compared to the backpropagation of Rumelhart et al. (1986).

In practice, the boundary between statistical and AI models is quite ambiguous. MARS can for instance belong to either of the two groups. MARS, as introduced by Friedman (1991), is a non-parametric regression based method which is able to automatically model non-linearity's and interactions between variables. MARS consist of a forward and backward phase. In the forward phase, the model is built. The built model is simplified in backward phase to prevent overfitting of the model on the training data. In contrast to MLR but similar to the ANN, MARS has the advantage that it does not need an assumption about the underlying functional relation between dependent and independent variables. Nalcaci et al. (2019) find the performance of the MARS superior to MLR models and competitive with the ANN for load forecasting. Since ANN and

MARS are non-parametric methods that do not need a pre-specified functional relation, both the model and the parameters need to be fitted on the training data. To prevent the non-parametric methods to lack power, a large part of our data is dedicated to training the models.

Load forecasting models can consist of a single stage or a sequence of stages. Advantages of a single-stage model are: all variables can interact, the model is simple to construction and the model is easy to use for forecasting. A multi-stage approach, also called a multi-model approach, has the advantage that the strengths of different methods can be combined to improve the forecast performance. Nelson, Hill, Remus, and O'Connor (1999) show the usefulness of multi-stage modelling for neural networks on load data. In contrast to the theory that the non-parametric method should be able to capture the (non-)linear seasonal pattern and weather information simultaneously, they find the forecasts of neural networks to be significantly more accurate if the data is deseasonalized before the relation with the weather variables is modelled. In later research, Zhang and Qi (2005) also conclude: ”... just as traditional statistical models, neural networks are not able to simultaneously handle many different components of the data well and hence data preprocessing is beneficial”.

Palit and Popovic (2006) state that the data preprocessing, or decomposition analyses of a time-series usually consists of detrending and deseasonalizing the data. If the load demand contains a significant trend or seasonal pattern, first removing the trend or seasonal pattern can simplify modeling and improve model performance. After detrending the data, seasonality is a dominant feature in the load demand time-series. Park, El-Sharkawi, Marks, Atlas, and Damborg (1991) and Lusis, Khalilpour, Andrew, and Liebman (2017) observe that the hourly time-series for load data contains daily, weekly and yearly seasonal patterns. There are various methods to deseason the hourly load data. Chen, Wang, and Huang (1995) use subsets of data and then estimate the parameters on each subset separately. The disadvantage of splitting the data into subsets is that it can lead to an abundance of models. An alternative method to model seasonal patterns is the use of explanatory variables. Hong et al. (2010) differentiate times of the day, week and year through dummy variables, which are equal to one on specific moments of the day, week or year and zero otherwise. Magnano and Boland (2007) use dummy variables to model the weekly seasonality, however use polynomial Fourier series for modeling the daily and yearly seasonal patterns in the load demand.

Besides a trend and seasonal pattern, Hong et al. (2010) conclude that national holidays, vacation periods as well as weather and economic variables impact the load demand. On a national holiday for instance, businesses, factories, and office buildings are mostly closed. Hong et al. (2010) find that the effect of a national holiday in the US is comparable with the effect of either a Monday, Saturday or Sunday. Due to a strong correlation between power consumption and weather variables such as temperature, humidity, wind speed, and cloud cover, Park et al. (1991) conclude that utilizing weather information can improve the accuracy of the forecasts. In contrast to Park et al. (1991), Magnano and Boland (2007) find that weather variables have little explanatory power. The difference in conclusions can be explained by the different moments of incorporation of the weather data as explanatory variable. Park et al. (1991) use weather data directly as explanatory variable for load demand, in contrast to Magnano and Boland (2007), who investigate the relation between deseasonalized load and weather variables. The model for deseasonalizing the load data already explains a significant amount of the variability of the electricity demand due to the weather variables, after which the explanatory power of the weather variables itself, is far smaller.

Since weather and economic variables are uncertain in the long-term and we want to prevent a look-ahead bias, the weather and economic variables are simulated. An average of the previous decades is however not defensible according to Hyndman and Fan (2009). This approach is not defensible since an average temperature profile understates the peaks and does therefore not represent the normal spread in weather. A second reason why the average weather profile may not lead to a representative load profile is due to the non-linear relationship between the load and weather variables. The solution of Hyndman and Fan (2009) is to use a double seasonal block bootstrap method, which captures the daily as well as annual seasonality of the weather variables, to generate more realistic input scenarios.

3 Data

The hourly load data in megawatt (MW) for Luxembourg is freely accessible from the European Network of Transmission System Operators for Electricity (ENTSO-E). ENTSO-E represents 42 electricity transmission system operators from 35 countries across Europe. Creos Luxembourg is the transmission system operator which provides the data for the Grand-Duchy of Luxembourg. Compared to other European countries, the load data of Luxembourg has the following advantages: the ENTSO-E network is the single power provider for all of Luxembourg; the data collection method has not changed over time and a single weather station is representative for the entire country because Luxembourg is the second smallest country of Europe with a surface of only 2586 km^2.

The load dataset starts at 0 AM 01/01/2006 local time and consists of hourly observations until 12 PM 31/12/2017, resulting in a period of 12 years, 4383 days or 105192 hours of data. 10 of the 105192 hourly load observations are missing, for which the average of the previous and next known load is assumed. The data is split into a training and test set. The data for model construction is the training set, which starts at 0 AM 01/01/2006 and ends at 12 PM 31/12/2014 (78888 hours). LTLF are made and assessed against the test data, which starts at 0 AM 01/01/2015 and ends at 12PM 31/12/2017 (26304 hours). Although more accurate weather forecasts for the first two weeks would have been available, this data is ignored in order to simulate identical data availability. This allows us to make forecasts for these first two weeks, as if it were LTLF.

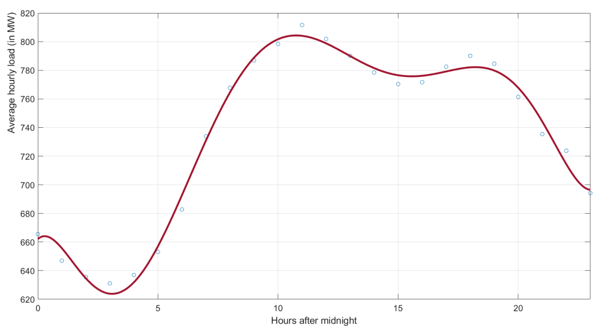

*(a) Daily seasonal pattern**

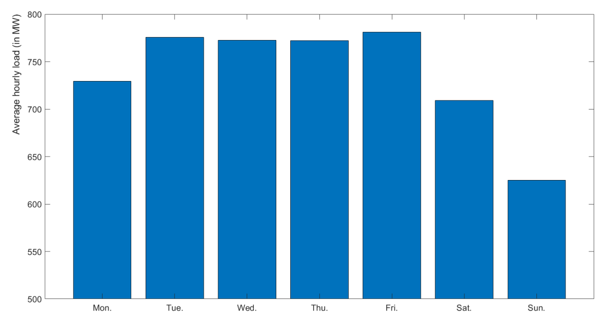

(b) Weekly seasonal pattern

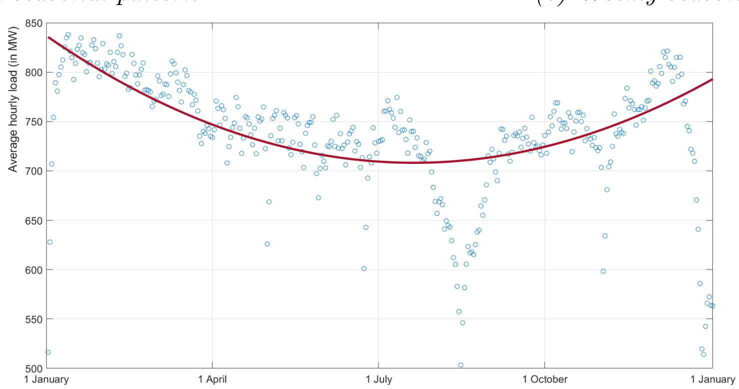

*(c) Yearly seasonal pattern***

*7-th degree polynomial fitting curve. ** 2-th degree polynomial fitting curve.

Figure 1: The average daily, weekly and yearly seasonal patterns of the hourly load demand in Luxembourg from 01/01/2006 until 31/12/2014.

The hourly load demand in Luxembourg contains daily, weekly and yearly seasonal patters. Figure 1a shows the average load demand at different hours of the day for the training data. The load demand is the lowest between midnight and 5 AM, after which the demand increases until approximately 10 AM. The average demand is maximal between 10 AM and 8 PM, after which it starts to decline. Figure 1b shows the weekly seasonal pattern, in which the average load demand on Monday, Saturday and Sunday is lower than on the other days of the week. The yearly seasonal pattern in Figure 1c shows that the average load demand is higher during winter months than during summer months. Spring and Autumn fall in between these periods of high and low average load demand.

The lines fitting the data in Figure 1a and 1c are 7-th and 2-th degree polynomial functions. These polynomial functions serve as explanatory variables (Section 5) and the degree of these polynomials is preferred over other polynomial degrees based on the fit of the average load demand and the cyclical nature of the function, with a small difference between the load value at start and end of a cycle. Since the explanatory variables for the weekly seasonal pattern consist of dummy variable instead of polynomial functions, Figure 1b represents the weekly seasonality in a bar chart instead.

The average load demand is lower on national holidays. The negative outlying observations in Figure 1c are mainly the consequence of national holidays and vacation periods. The lower demand at the end of December and at the beginning of January may be explained by Christmas season. The demand decrease from mid- July until the end of August could be the result of summer vacations and the construction break. The impact of national holidays is illustrated by the outlying observation on 1 November, due to All Saints' Day and the lower demand on 23 June, which is the consequence of National Day. The reduction in load demand on the days surrounding national holidays could be the result of extended holiday activities (Hong et al., 2010).

Meteostat provides the hourly weather data and is freely online accessible for high-frequency data on weather and climate statistics worldwide. The only weather station in the Meteostat database in Luxembourg is at Luxembourg Airport. Since this station contains many missing values and has no hourly data for 2011, the closest weather station in Trier-Petrisberg (Germany) is used. Trier-Petrisberg is roughly 10 km from the border of Luxembourg and 50 km from the city-centre of Luxembourg. The hourly weather data consist of: the temperature (in $°C$), the dew point (in $°C$), relative humidity (in %), precipitation (in mm), the wind speed (in km/h) and the air pressure (in hPa) (Appendix 9.1.1). The amount of missing values for the weather variables is between 0.041

and 0.165 percent, for which an average of the two adjacent observations is assumed. We expect the influence of the missing load and weather values to be negligible, since the amount of missing values is small and both time-series are continuous for which an average of adjacent data points provides an reasonable approximation.

Yahoo! Finance provides an economic metric for Luxembourg, which is the DAX-index. The DAX-index consists of 30 major German companies. The DAX-index provides a good measure for economy of Luxembourg because Luxembourg's economy is highly dependent on the economy of Germany. German Federal Foreign Office (2020) state that Germany is Luxembourg's main economic partner, accounting for approximately 27% of total foreign trade in 2016.

4 Methodology

The first-stage model starts with modelling seasonal patterns, after which calendar events are incorporated in the second stage. In the last stage, the remaining effects of economic and weather variables are modelled. The first stage model is given by $Y_1 = f(X_1) + Y_2$, in which Y_1 is the hourly load demand and X_1 consists of the explanatory variables to model seasonal patterns. The residuals from the first stage (Y_2) represent the deseasonalized load and are the dependent variable in the second stage. The second stage removes the effects of national holidays and vacation periods (X_2) from the deseasonalized load, given by $Y_2 = g(X_2) + Y_3$. In the third stage investigates the relationship between weather and economic variables (X_3) and the residuals from the second model (Y_3). This third and last stage model is given by $Y_3 = z(X_3) + \varepsilon$, in which ε represents the unexplained variation of the load demand due to randomness and other, overlooked variables. The functions $f(.)$, $g(.)$ and $z(.)$ in the sequence of three stages are all estimated using MLR, ANN and MARS models. The functions do not necessarily have to be constructed using the same model, such that the strengths of different models in different stages can be combined.

The explanatory variables to model the effects of seasonal patterns and calendar effect are known with certainty for the future, which we therefore directly use for out-of-sample forecasting. Weather and economic variables are however uncertain in the long-term. By simulating different input scenarios using double seasonal block bootstrap and averaging the resulting set of forecasts, we construct out-of-sample point forecasts.

4.1 Multiple Linear Regression (MLR)

A simple linear regression has a single explanatory variable, in contrast to MLR which has multiple explanatory variables. The MLR model is given by $Y = X\beta + \varepsilon$, in which Y is a Tx1 vector of the dependent variable, ε is a Tx1 vector of the residuals and the TxK matrix X contains for each of the T data observations, the value of K explanatory variables. The coefficients in the Kx1 β vector are estimated by Ordinary Least Squares (OLS) and measure the effect of each explanatory variable after taking the effects of the other predictors into account.

The effect of a predictor variable may depend on the value(s) of some other predictor variable(s). Nalcaci et al. (2019) use a MLR model which does not allow for interaction between the explanatory variables. Since we expect the variables to be interacting and possibly non-linear, we use a simple and an extended MLR model. The explanatory variable in the simple model consists of only an intercept term and non-interacting linear explanatory variables. The extended MLR contains, besides the intercept term and the non-interacting linear explanatory variables, squared terms as well as interacting terms, which consist of the product of two distinct predictors. Based on the AIC-criteria, we add explanatory variables using forward selection, after which backward elimination investigates if some of the variables can be removed due to a lack of explanatory power.

4.2 Artificial Neural Network (ANN)

ANN is a neural network based on a biological brain, which can model complex and possibly non-linear relationships between the dependent output variable Y and the K explanatory input variables in X, given by $Y = h(X) + \varepsilon$.

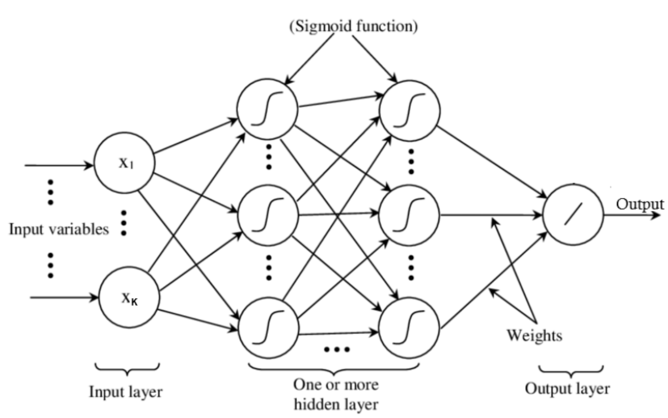

Figure 2: A scheme for the ANN.

Figure 2 graphically illustrates how the input nodes are connected through a network of hidden layers to output nodes, where the connections between nodes correspond to weights. Gardner and Dorling (1998) describe a feed-forward ANN, also known as a multilayer perceptron. The ANN model starts with the original input variables $X = [x_1, ..., x_K]$ in the input layer. A node k in every subsequent layer $j \in \{1, ..., n\}$ gets as input, the output of the $p_{(j-1)}$ nodes in layer $j-1$, given by $q_{(j-1)} = [q_{(j-1,1)}, ..., q_{(j-1,p_{(j-1)})}]$. In each node, the input is multiplied with a vector of weights which leads to $z_{(j,k)} = \sum_{i=1}^{p_{(j-1)}} w_{(j-1,i)} q_{(j-1,i)} + b_{(j,k)}$. $b_{(j,k)}$ denotes the external bias of node k in layer j and acts as a constant which helps the model to fit the given data. Finally, before passing the information to the nodes in the next layer, an activation function φ transforms the weighted sum $z_{(j,k)}$. If the function is linear, the multilayer perceptron would only be able to model linear functions. Since we want to be able to capture non-linear relationships between the explanatory and independent variables, the activation function is the differentiable logistic sigmoïd function. The resulting output of node k in layer j is then given by $q_{(j,k)} = \varphi(z_{(j,k)}) = \dfrac{e^{z_{(j,k)}}}{1+e^{z_{(j,k)}}}$. The n-th layer is the output layer and has a linear activation function Φ instead, because the target output, which represents electrical load, is not on an interval between 0 to 1. Repeating this information processing over all the nodes in every layer results in the following estimate of the dependent variable Y:

$$\hat{Y} = q_{(n)} = \Phi(z_{n,1}) = \Phi\left(\sum_{i=1}^{p_{(n-1)}} w_{(n-1,i)} \varphi(z_{(n-1,i)}) + b_{(n,1)}\right) = ...$$
$$... = \Phi\left(\sum_{i=1}^{p_{(n-1)}} w_{(n-1,i)} \varphi(...\varphi(\sum_{h=1}^{p_{(1)}} w_{(1,h)} \varphi(\sum_{l=1}^{K} w_{(0,l)} x_l + b_{(1,h)}) + b_{(2,u)}) + ...) + b_{(n,1)}\right),$$

in which $u \in \{1, ..., p_{(2)}\}$ is a node from the second hidden layer.

The weights between nodes determine the estimate and are optimized through an iterative supervised training process. In supervised training, the objective is to tune the weights in the network such that the network performs a desired mapping of input to output. The weights are randomly initialized, after which we use the Levenberg-Marquardt backpropagation algorithm as in Hagan and Menhaj (1994). The Levenberg-Marquardt backpropagation algorithm changes the weights depending on the derivative of the loss function of the prediction error (Appendix 9.2.1). The methodology has a high convergence rate and a limited calculation time, which allows for the use of the full data set for a single adjustment of the weights. The process of training the ANN continues until the loss function of the validation set fails to decrease for six successive iterations. The validation set consists of a randomly selected 25% of the training set and prevents overfitting of the ANN model. Since the number of training observations is large and we use 25% of the training data as validation set, we do not add more restriction to the validation set.

The best method to set the number of nodes and hidden layers is testing different settings, since Karsoliya (2012) finds the tuning of these parameters problem specific, such that no general best setting is available. We found it optimal in our models to set the number of hidden layers at two and the number of nodes per hidden layer at fifteen. Smaller neural networks are less accurate, but neural networks with more nodes do not improve the forecasts accuracy significantly and can result in overfitting.

4.3 Multivariate Adaptive Regression Splines (MARS)

Friedman (1991) introduces the MARS method, which is a generalization of a linear step-wise regression. MARS models the relationship between the dependent variable Y and the explanatory variables in the matrix $X = [x_1, ..., x_K]$ in the following form: $Y = b(X) + \varepsilon$. The estimation of the $b(.)$ function is $\hat{b}(X) = \sum_{i=1}^{M} c_i B_i(X)$, in which c_i is the coefficient corresponding to the basis function $B_i(X)$. The coefficient is determined using OLS and a basic function is either a constant or a (product of) hinge function(s). A hinge function, also known as a two-sided truncated power basis (Friedman, 1991), is given by $[\pm(x_j - \tau_j)]_+$, in which the $+$ symbol specifies that only the positive parts are used. $[(x - \tau)]_+$ can therefore be rewritten as $\max\{0,\, x - \tau\}$ and $[-(x - \tau)]_+$ as $\max\{0,\, \tau - x\}$. A basis function has the following form $B_i(X) = \Pi_{j=1}^{K_i}[\pm(x_j - \tau_j)]_+$, in which K_i represents the number of variables involved in the i-th basis function and τ_j is a knot. A knot is a point on the domain of a variable, where the $\pm$-sign in the hinge function switches from positive to negative or vice versa (Appendix 9.2.2, Figure 5).

MARS implements a sequence of two phases, namely a building and backward phase. In the building phase, the estimated function starts with only a single basis function which consist of a constant ($\hat{b}(X) = c_0$). This function is then repeatedly extended with a pair of basis functions until the maximum of basis functions is reached ($M = M_{max}$) or the Generalized Cross-Validation (GCV) has not decreased significantly. GCV is a performance measure for the MARS model, which depends on the model complexity μ. The $GCV(\mu)$ is given by:

$$\sum_{t=1}^{T} \frac{(y_t - \hat{f}_\mu(x_t))^2}{(1 - M(\mu)/T)^2},$$

in which $M(\mu)$ represents the effective number of parameters and is calculated as $M(\mu) = u + d \times \lambda$.

Here, u represent the number of basis functions, λ is the number of knots and d represent the cost for each extra knot. Under the assumption that $M(\mu) < T$ and that all other components stay the same, a higher $M(\mu)$ corresponds to a more complex model and therefore a higher GCV. In each iteration, MARS adds the pair of basis functions which leads to the maximum reduction in GCV. A pair of basis functions, instead of a single basis function, is added because both parts of the hinge function ($[+(x_j - \tau_j)]_+$ and $[-(x_j - \tau_j)]_+$) are multiplied with one of the basis functions in the model. The new hinge function depends on which knot locations are allowed per variable. To reduce computation time and to lower the local variance of estimates, only a subset of knot locations in the domain of a variable is considered (Appendix 9.2.2). After the building phase, we apply a backwards stepwise procedure as in Friedman (1991) to prevent overfitting by decreasing the complexity while maintaining a relative good fit. In the backward phase, MARS deletes the single basis function which maximizes the decrease in GCV and continues as long as the decrease in GCV is significant.

The cost of extra knots (d) is set at 3, which lies in the middle of the [2,4] interval which Friedman (1991) advises. Moreover, the maximum number of basis functions in the forward phase (M_{max}) should be approximately twice the amount of nodes in the model with the lowest GCV. The maximum allowed number of basis function in the forward phase is therefore set at 100. The maximum number of interacting hinge functions is 3, which we find the best compromise between the fit of the data on the one hand and simplicity and calculation time on the other hand.

4.4 Double seasonal block bootstrap

Bootstrapping involves random re-sampling of historical data. Block bootstrap aims to replicate the correlation in the data by re-sampling blocks of data instead of individual data points. Hyndman and Fan (2009) state that it is important to preserve any seasonal or trend patterns as well as inherent serial correlation. The weather data contains no unidirectional trend but it contains a daily and yearly seasonal pattern (Appendix 9.1.1). To preserve both the daily and yearly seasonal pattern, we use a variant of the double seasonal block bootstrap of Hyndman and Fan (2009) and combine the sampled blocks of data to generate one long input scenario.

The length of each block is a multiple of the length of the daily seasonal period. Each block consist of α whole days or $\alpha * 24$ hourly observations to preserve the daily pattern. To preserve the yearly pattern, blocks in the generated input scenario start on the same day of the year as the historical data or $\pm\lambda$ days, where λ is an independent uniformly distributed integer in the interval [-14,14]. To divide each year in 4 blocks, α is 91 or 92 days. Blocks of this length are long enough to capture serial correlations within these blocks, however short enough to allow sufficient series to be generated. Moreover, the amount of unrealistically large jumps between blocks in the new scenario is small, which should prevent the jumps to impact the forecast performance significantly.

5 Explanatory variables

Stage 1: Seasonal patterns

The load demand in Luxembourg contains no clear increasing or decreasing trend over the years, so a trend correction is not needed. Therefore, the hourly load demand is only deseasonalized. The seasonality in the hourly load demand consist of a daily, weekly and yearly seasonal pattern (Section 3). Based on in-sample performance and autocorrelation in the residuals, different combinations of dummy and polynomial variables are evaluated. The resulting explanatory variables in the first-stage models consist of: a constant, two polynomial terms and three dummy variables.

The standardized 7-th degree polynomial from Figure 1a captures the daily seasonal pattern. The standardized quadratic trend-line from Figure 1c is the second explanatory polynomial variable and captures the yearly seasonal pattern. The three dummy variables differentiate different days of the week. Monday, Saturday and Sunday each get a separate dummy variable, which is equal to one on the specific day of the week and zero otherwise. We choose to include variables for Monday, Saturday and Sunday specifically, because Figure 1b shows that the average load demand on these days is lower compared to the remaining days of the week.

Stage 2: National holidays and vacation periods

Hong et al. (2010) compare the effect of a national holiday in the United States to either a Saturday, Sunday or Monday. We use dummy variables instead, because Luxembourg has different national holidays than the United States and it does not require potentially inaccurate assumptions about which weekday is comparable to which national holiday. In the second-stage, each of the following extraordinary days are separated from the ordinary days with a dummy variable: national holidays, day before and after a national holiday, Christmas Season, peak summer and late summer. The dummy to model the effect of national holidays is equal to one on: New Year, Easter, Labour Day, Ascension Day, White Monday, National Day, Assumption Day, All Saints' Day, Christmas Day and Boxing Day. The specific dates of Christmas season differ each year, but are generally speaking from the weekend before Christmas until the weekend after New Year. For the peak summer, we use the construction break. Stopping construction affects consumption which reduces power generation needs and it falls together with school vacations. Late or after summer starts directly after the end of the peak summer and usually covers the last two weeks of August.

Even after deseasonalizing the load demand, the effect of extraordinary days can dependent on the time of the year, day of the week and hour of the day. For instance, the effect of a national holiday in a weekend can be smaller than on a weekday since many businesses were already closed. Therefore, we include the two polynomial terms from the first-stage as well as a single dummy to differentiate weekends from weekdays. A combination of time-dependent and calendar variables can be informative. The time-dependent variables should have no explanatory power on themselves, since these effects are already modelled in the first-stage model.

Stage 3: Weather and economic variables

The hourly weather data of the Meteostat database consist of: the temperature (in $^{\circ}C$), the dew point (in $^{\circ}C$), precipitation (in mm), the wind speed (in m/s) and the air pressure in hectopascal (hPa). Alongside the Meteostat variables, the set of explanatory weather variables consists of: the maximum and minimum temperature in the last 24 hours, the difference between minimum and maximum temperature in last 24 hours, an average temperature at the same time of a day over the last seven days, precipitation in the last 24 hours, Heating Degree Day (HDD) and Cooling Degree Day (CDD).

HDD and CDD are designed to quantify the demand for energy needed to heat or cool a building. They are defined relative to a base temperature, which is the outside temperature below or above a building needing heating or cooling. European Environment Agency (2019) sets the base temperature in the European Union at $15.5^{\circ}C$ and $22.0^{\circ}C$ respectively. If avg_temp is the average temperature in the last 24 hours, then HDD at a certain hour is $\max\{0, 15.5 - avg\_temp\}$ and CDD is $\max\{0, avg\_temp - 22.0\}$.

The economic explanatory variable in the third-stage model is the simple stock return of the DAX-index over the last month. The stock return is more appropriate than the DAX-index itself, since the models do not correct for the predominate upward trend of the DAX-index. The effect of changing economic circumstances has a delayed effect on the load demand, which is reason to use the stock return over an entire month. Lastly, the third-stage set of explanatory variables contains the time-dependent variables from the second stage. The effects of weather variables on the season- as well as calendar-adjusted load demand can dependent on the time. For instance, the effect of a cold weekend day on which many people are at home, can differ from a cold weekday on which most people are working.

6 Results

The first stage models the daily, weekly and yearly seasonal patterns in the hourly load demand. Table 1 contains the forecast performance of the MLR, extended MLR with interacting and quadratic terms, ANN and MARS models, in which the performance is based on the R^2_{adj}, $RMSE$ and $MAPE$ forecasts criteria (Appendix 9.1, Table 6). Extending the MLR model with quadratic as well as interacting terms, improves the forecast performance. The $MAPE$ for the training data reduces from 11.15% to 10.58% and the $MAPE$ for the out-of-sample test dataset reduces from 11.14% to 10.76%. Compared to the (extended) MLR model, ANN and MARS models incorporate more of the information contained in the explanatory variables for modelling seasonality. For the training and test dataset, the R^2_{adj} is closer to one and both the $RMSE$ and $MAPE$ are closer to zero. The MARS model is especially suitable for deseasonalizing the load demand, since it performs best on all criteria.

Table 1: Forecasts performance of MLR, extended MLR, ANN and MARS models for modelling daily, weekly and yearly seasonality in first stage. Training data from 01/01/2006 until 31/12/2014, test data from 01/01/2015 until 31/12/2017. The best performance is highlighted in bold.

	MLR		ext. MLR		ANN		MARS	
Criteria	Train	Test	Train	Test	Train	Test	Train	Test
R^2_{adj}	0.431	0.292	0.479	0.329	0.573	0.383	**0.608**	**0.455**
$RMSE$	96.56	95.96	92.39	93.41	83.65	89.53	**80.11**	**84.19**
$MAPE$ (%)	11.15	11.14	10.58	10.76	9.57	10.32	**9.19**	**9.59**

Table 2 compares the training performance of the first-stage ANN and MARS models on extraordinary days based on the average residual (Avg. Resid), $RMSE$ and $MAPE$. The average residuals are negative in vacation periods, on national holidays and on the days surrounding national holidays. This indicates that the ANN and MARS model overestimate the load demand on the extraordinary days, which is a consequence of the lower average load demand on these extraordinary days (Section 3). On ordinary days the $RMSE$ of the MARS model is 76.90, which increases on extraordinary days to a minimum of 80.09 and maximum of 142.6. The ANN and MARS models underestimate the load demand on ordinary days, which can be the result of the overestimation on extraordinary days. Moreover, it is remarkable that the forecast errors of the ANN model on extraordinary days are higher than of the MARS model.

Table 2: Forecasting performance on national holidays and in vacation periods for the first-stage ANN and MARS models, 01/01/2006 until 31/12/2014.

	ANN	MARS	ANN	MARS	ANN	MARS
Criteria	National holiday		± National holiday*		Peak summer	
Avg. Resid. (MW)	-110.2	-81.04	-49.46	-19.59	-46.16	-46.15
$RMSE$	152.0	142.6	111.0	93.20	79.38	80.09
$MAPE$ (%)	24.42	21.96	15.87	12.70	10.61	10.69
	Holiday season		Late summer		Ordinary	
Avg. Resid. (MW)	-78.67	-22.76	-45.29	-37.92	11.75	8.16
$RMSE$	122.0	94.43	81.25	80.97	79.20	76.90
$MAPE$ (%)	18.37	13.10	11.81	11.46	8.63	8.41

*Day before and day after national holidays.

Table 3: Forecasts performance of MLR, extended MLR, ANN and MARS models for modelling national holidays and vacations in the second stage. Training data from 01/01/2006 until 31/12/2014, test data from 01/01/2015 until 31/12/2017. The best performance is highlighted in bold.

Stage 2:	None*		MLR		Ext. MLR		ANN		MARS	
	Train	Test	Train	Test	Train	Test	Train	Test	Train	Test
Stage 1: MARS										
R^2_{adj}	0.608	0.455	0.630	0.474	0.644	0.477	**0.665**	**0.481**	0.665	0.473
$RMSE$	80.11	84.19	77.89	82.69	76.40	82.47	**74.10**	**82.13**	74.12	82.74
$MAPE$ (%)	9.19	9.59	8.88	9.41	8.69	9.35	8.42	**9.29**	**8.42**	9.36
Stage 1: ANN										
R^2_{adj}	0.573	0.383	0.619	0.432	0.633	0.442	**0.678**	**0.472**	0.674	0.470
$RMSE$	83.65	89.53	79.03	85.92	77.56	85.18	**72.64**	**82.82**	73.05	82.99
$MAPE$ (%)	9.57	10.32	8.96	9.79	8.76	9.66	**8.23**	9.40	8.30	**9.40**

*First-stage results from Table 1.

The second stage models the relationship between the deseasonalized load from the first stage and the effects of national holidays and vacation periods. Based on the R^2_{adj}, $RMSE$ and $MAPE$, Table 3 shows the increase in forecast performance of second-stage MLR, extended MLR, ANN and MARS models compared to the first-stage MARS and ANN models. Generally speaking, distinguishing national holidays and vacation period enhances the forecasts. Similarly to the first stage, the performance of the extended MLR is slightly better than the basic MLR. The ANN and MARS models again result in more accurate forecasts compared to the (extended) MLR. This can be the result of sub-optimal specification of the (complex) functional relationships between dependent and explanatory variables in the (extended) MLR model.

The performance of any first- and second-stage ANN or MARS model combination is fairly similar. We choose to further investigate the first- and second-stage ANN model (ANN-ANN), because the R^2_{adj} is, with a value of 0.678, closest to one for the training dataset. Table 4 shows the success of the ANN-ANN model in distinguishing national holidays and vacations periods from ordinary days. The average residual on extraordinary days is closer to zero compared to the first-stage results in Table 2. Based on the $RMSE$ for both the training and test data, the ANN-ANN model forecasts even more accurately on extraordinary days than on ordinary days.

Table 4: Forecasting performance on national holidays and in vacation periods after deseasonalizing and incorporating calendar effects with first- and second-stage ANN models. Training data from 01/01/2006 until 31/12/2014, test data from 01/01/2015 until 31/12/2017.

	Train	Test	Train	Test	Train	Test
Criteria	National holiday		± National holiday*		Peak summer	
Avg. Resid. (MW)	-0.126	0.368	0.330	-13.31	0.833	4.324
$RMSE$	68.70	79.59	71.49	79.63	57.98	73.16
$MAPE$ (%)	10.04	10.72	9.33	10.80	7.29	9.67
	Holiday season		Late summer		Ordinary	
Avg. Resid. (MW)	0.671	-25.76	-0.258	0.592	0.020	-11.84
$RMSE$	64.78	72.15	58.80	65.97	73.06	83.36
$MAPE$ (%)	8.53	10.46	7.88	8.81	8.25	9.44

*A day before and after national holidays.

The third-stage model investigates the relation between the seasonal- and calendar-adjusted load demand and economic and weather variables. Out of the abundance of weather variables from Section 5, a pre-selection of variables is made in order to prevent multicollinearity. In the pre-selection, we evaluate different sets of explanatory variables based on the in-sample performance and by looking at which variables are incorporated in the MARS model. After the pre-selection, the set of explanatory weather variables for Luxembourg consist of: HDD, precipitation in the last 24 hours, temperature and dew point.

Table 5 contains the third-stage forecast performance of the MLR, extended MLR, ANN and MARS models using the season- and calendar adjusted load from the ANN-ANN model. The training performance of the third-stage (extended) MLR model has not improved significantly compared to the second-stage ANN-ANN forecasts, which indicates that these methods do not find weather and economic data informative. An explanation could be that the relationship between the already adjusted load demand and the economic and weather variables is too complex for the (extended) MLR model (Hyndman & Fan, 2009). In contrast to the (extended) MLR model, the third-stage ANN and MARS models enhance the in-sample forecasts. The ANN-ANN model has a $MAPE$ of 8.23%, which the third-stage ANN and MARS models reduce to 6.49% and 6.96% respectively. The total effect of the weather variables on the load demand is probably higher than incorporated in the third-stage model, since a part of the effects of weather variables is already incorporated in the first-stage deseasonalizing model (Magnano & Boland, 2007). If one is in possession of weather data and the load demand is already adjusted for seasonality, we still recommend to incorporate weather variables since the third-stage ANN and MARS models enhances the in-sample forecasts.

To deal with the uncertainty of weather and economic variables for out-of-sample LTLF, 1000 different scenarios are generated using double seasonal block bootstrap. Some of the 1000 input scenarios improve the LTLF, however the use of the average of the 1000 different scenario forecasts does not improve the LTLF performance (Table 5: Test data). The constructed three-stage ANN and MARS models can however be useful for other application such as 'what-if' analyses.

Table 5: Forecasting performance of MLR, extended MLR, ANN and MARS models in the third stage, where the relationship between economic and weather variables and the residuals from first- and second-stage ANN model is investigated. Training data from 01/01/2006 until 31/12/2014, test data from 01/01/2015 until 31/12/2017. Estimates on the test data for the (extended) MLR are omitted, since the use of economic and weather variables do not improve model performance on the training data. The best training performance is highlighted in bold.

	Target*		MLR		ext. MLR		ANN		MARS	
Criteria	Train	Test	Train	Test	Train	Test	Train	Test	Train	Test
R^2_{adj}	0.678	0.472	0.681	-	0.684	-	**0.797**	0.466	0.766	0.471
$RMSE$	72.64	82.82	72.32	-	71.99	-	**57.73**	83.33	61.88	82.96
$MAPE$ (%)	8.23	9.40	8.19	-	8.14	-	**6.49**	9.45	6.96	9.41

*Forecasts from the ANN-ANN model (as in Table 3).

7 Conclusion

Electric load forecasts are vital to ensure reliable power supply. This paper investigates three-stage Multiple Linear Regression (MLR), Artificial Neural Network (ANN) and Multivariate Adaptive Regression Splines (MARS) models for hourly long-term load forecasting in Luxembourg. The hourly long-term forecasts are suitable for many load forecasting problems such as: investment decisions, operations and maintenance, transmission and distribution planning as well as demand management. The explanatory variables incorporated in the three stages consist of: seasonal patterns, calendar effects as well as weather and economic variables. In each stage, the non-parametric ANN and MARS models result in more accurate forecasts in comparison to the parametric (extended) MLR model, especially when the relation between variables seems to be more complex. In contrast to the MLR method, ANN and MARS models are able to find functional relationships between weather and economic variables on the one hand and seasonal- as well as calendar-adjusted load on the other hand. The values of the economic and weather explanatory variables are however unknown in the long-term. A set of 1000 weather and economic scenarios is generated, using double seasonal block bootstrap. Each scenario leads to hourly forecasts for the entire test dataset. In contrast to some of the scenarios, the average of the 1000 load forecasts does not enhance the forecast performance. The constructed three-stage models are however useful in other applications, such as 'what-if' analyses.

8 Recommendations

Further research can investigate if a simplified model can be developed through merger of stages. An example is to incorporate the seasonal, calendar, economic and weather patterns in a single stage. The effect of the bootstrap generated economic and weather scenarios may then be able to enhance the out-of-sample forecasts. New research can also investigate if the forecasts can be enhanced by differentiating types of consumers. ENTSO-E serves different types of energy consumers such as residents, businesses, and industries. Since effects of the explanatory variables on the energy demand are likely to be consumer specific, a model dedicated to only one sector may enhance the forecast performance. To prevent a look-ahead bias, we omitted past load as explanatory variable. The influence on model performance by including past load as explanatory variable can be investigated, possibly in combination with short- instead of long-term load forecasts.

9 Appendix

9.1 Additional results

Table 6: Explanation of performance measures.

Name	Explanation	Goal	Formula
Avg. Resid.	Average residual	Close to zero	$\frac{1}{T}\sum_{t=1}^{T}(y_t - \hat{y}_t)$
R^2_{adj}	Percentage of explained variation	Close to one	$1 - \left(\frac{\sum_{t=1}^{T}(y_t - \hat{y}_t)^2}{\sum_{t=1}^{T}(y_t - \bar{y}_t)^2}\right)\left(\frac{T-1}{T-p-1}\right)$
$RMSE$	Square root of mean squared error	Close to zero	$\sqrt{\frac{1}{T}\sum_{t=1}^{T}(y_t - \hat{y}_t)^2}$
$MAPE$	Average magnitude of percentage errors	Close to zero	$\frac{1}{T}\sum_{t=1}^{T}\left\lvert\frac{y_t - \hat{y}_t}{y_t}\right\rvert$

T represents the amount of observations and p corresponds with the number of parameters in a model.

Table 7: Performance of the first-stage ANN and MARS models on different times of the day, week and year. Period: 01/01/2006 until 31/12/2014.

	ANN				MARS			
Season	Summer	Winter	Autumn	Spring	Summer	Winter	Autumn	Spring
R^2_{adj}	0.582	0.550	0.556	0.524	0.583	0.679	0.560	0.512
$RMSE$	78.74	92.14	82.26	80.97	78.66	77.79	81.92	81.97
$MAPE$ (in %)	9.59	10.17	9.55	9.00	9.53	8.57	9.52	9.11
Weekday	Monday	Saturday	Sunday	Rest	Monday	Saturday	Sunday	Rest
R^2_{adj}	0.610	0.340	0.305	0.496	0.635	0.368	0.278	0.553
$RMSE$	83.40	80.43	69.72	87.60	80.65	78.68	71.02	82.45
$MAPE$ (in %)	9.65	9.42	9.38	9.64	9.30	9.23	9.44	9.08
Hours	0-6	6-12	12-18	18-24	0-6	6-12	12-18	18-24
R^2_{adj}	0.318	0.578	0.514	0.453	0.365	0.614	0.559	0.500
$RMSE$	81.96	83.98	84.14	84.49	79.07	80.32	80.22	80.83
$MAPE$ (in %)	10.74	9.34	8.92	9.29	10.31	9.00	8.54	8.89

9.1.1 Seasonal patterns in weather data

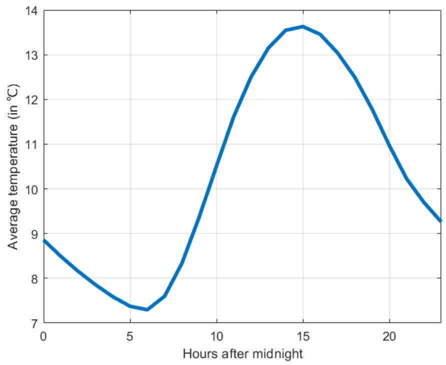

(a) Temperature

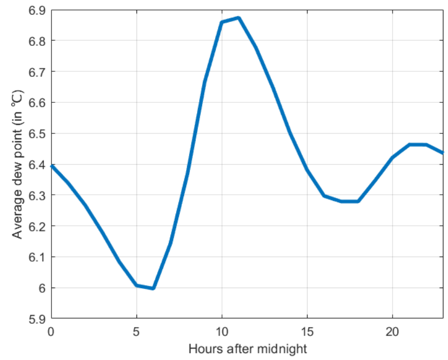

(b) Dew point

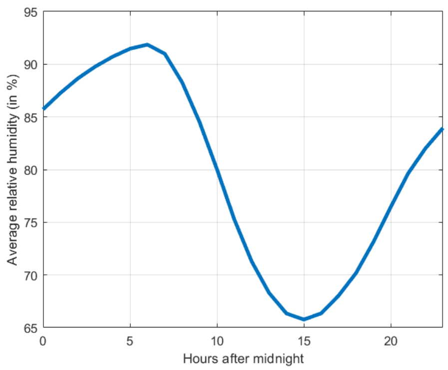

(c) Relative humidity

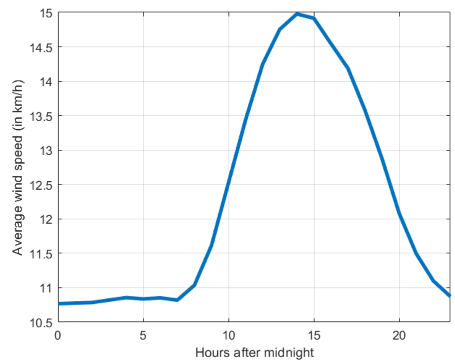

(d) Wind speed

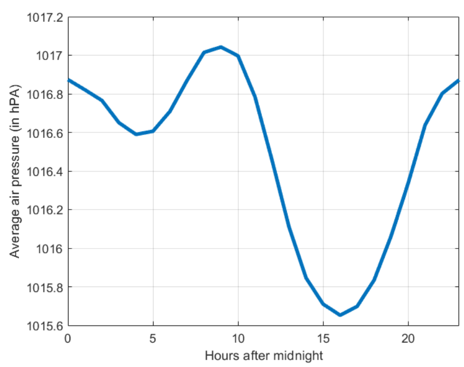

(e) Air pressure

Figure 3: Daily seasonal pattern of weather variables in Trier-Petrisberg based on average hourly data, starting at 01/01/2006 and ending on 31/12/2014. Lines connect data points directly and precipitation is omitted due to a lack of daily seasonal pattern.

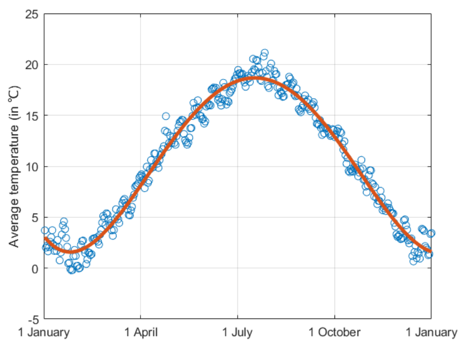

(a) Temperature

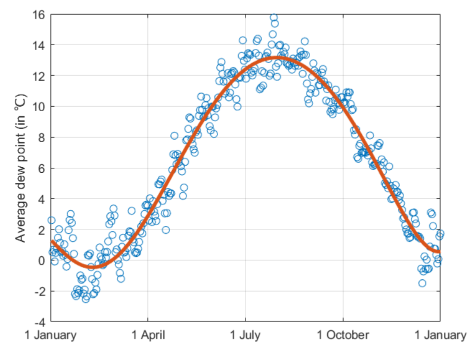

(b) Dew point

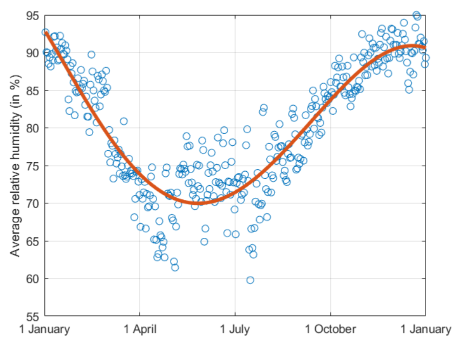

(c) Relative humidity

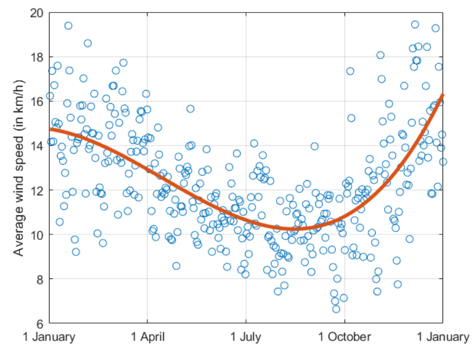

(d) Wind speed

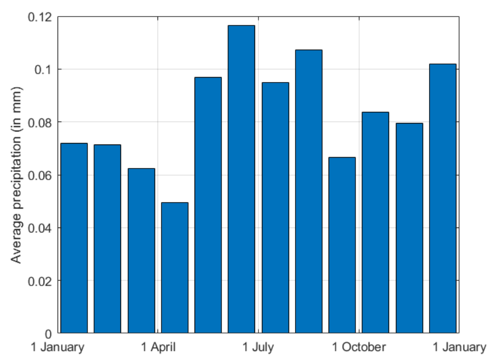

(e) Precipitation

Figure 4: Yearly seasonal pattern of weather variables in Trier-Petrisberg based on average daily data, starting at 01/01/2006 and ending on 31/12/2014. Air pressure is omitted due to a lack of yearly seasonal pattern.

9.2 Additional methodology

9.2.1 Levenberg-Marquardt backpropagation

In the Levenberg-Marquardt backpropagation algorithm of Hagan and Menhaj (1994), the loss function of sum squared errors is given by $V(w) = \sum_{i=1}^{T} \varepsilon_i^2(w) = \varepsilon'\varepsilon = \sum_{i=1}^{T}(y_t - \hat{y}_t)^2$, in which T is the number of observations and $V(w)$ is the loss function to minimize, with respect to the vector w which contains n weights. As in quasi-Newton methods, the Levenberg-Marquardt algorithm approximates the second-order derivative of the loss function instead of computing the real Hessian matrix, which reduces the computation time. If J is the Jacobian matrix with the first derivatives of the network error with respect to the weights and biases is given by

$$J(w) = \begin{bmatrix} \frac{\partial \varepsilon_1(w)}{\partial w_1} & \dots & \frac{\partial \varepsilon_1(w)}{\partial w_n} \\ \vdots & & \vdots \\ \frac{\partial \varepsilon_N(w)}{\partial w_1} & \dots & \frac{\partial \varepsilon_N(w)}{\partial w_n} \end{bmatrix},$$

then the Hessian matrix is approximated by $\hat{H} = J'J$ and the gradient is computed as $g = J'e$.

After calculation of the gradient and approximation of the Hessian matrix, the weights in the neural network are adjusted. The new weights are given by $w_{new} = w_{old} - [\hat{H} + \mu I]^{-1} g$, in which the scalar μ is a 'damping parameter' which essentially determines the method used to update the weights. If μ is large, the Levenberg-Marquardt backpropagation is essentially using gradient descent. When $\mu \approx 0$, the algorithm uses the Gauss-Newton method to update the weights instead. The 'damping parameter' is initialized with a large value so the method starts with gradient descent. Gradient decent updates the weights in the steepest-decent direction, without incorporating second order derivatives. Gauss-Newton updates the weights by incorporating an estimate of the Hessian matrix. The Gauss-Newton algorithm may converge slowly or not at all, if the initial guess is far from the minimum or the Hessian matrix is ill-conditioned. Far away from the minimum, the Levenberg-Marquardt method therefore acts more like a gradient-descent method. When the parameters are close to their optimal value, the Levenberg-Marquardt method acts like the Gauss-Newton method. After each iteration, μ is adjusted by either multiplying or dividing by $\beta = 10$. When the loss function decreases, μ is divided by β and if a tentative step increases the loss function, μ is multiplied by β.

9.2.2 Knot locations

In this paper, we use the knot placement algorithm of Friedman (1991). A knot placing algorithm lowers the local variance of the estimates, which makes the method resistant to runs of positive or negative error values between knots and it reduces the calculation time significantly. The knot locations are determined for each variable individually and require a minimum number of observation in between. The variance of the function estimates is especially high near the end of the domain of a variable, due to the lack of constraints on the fit at the boundaries. The minimum observations between the extreme knots and the corresponding interval ends are given by: $3 - \log_2(\frac{\alpha}{n})$, in which we set $\alpha = 0.05$ and n denotes the total number of explanatory variables under investigation. The minimum amount of observations for the remaining knots, which are in between the extreme knots locations, is given by $-\log_2(-\frac{1}{nN_m}\ln(1-\alpha))/2.5$, in which N_m is then number of positive observations in the m-th basis function.

In the third-stage model, the minimum observations between two knots is set at 500 instead. The knot placements in third-stage model needs to be adjusted, because the knot placement of Friedman (1991) allows for too many knots locations, which results in unfeasible long computation time. The first- and second-stage models do not need this adjustment, because a significant part of the explanatory variables in these stages consists of dummy variables. Since dummy variables only contain two values, the total number of knot location to evaluate remains feasible.

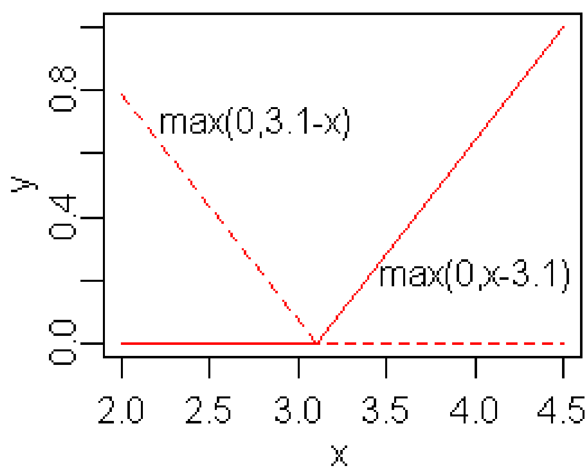

Figure 5: A mirrored pair of hinge functions with a knot at x=3.1.

References

Çevik, A., Weber, G.-W., Eyüboğlu, B. M., Oğuz, K. K., Initiative, A. D. N., et al. (2017). Voxel-MARS: a method for early detection of Alzheimer's disease by classification of structural brain MRI. *Annals of Operations Research*, *258*(1), 31–57.

Chen, J.-F., Wang, W.-M., & Huang, C.-M. (1995). Analysis of an adaptive time-series autoregressive moving-average (ARMA) model for short-term load forecasting. *Electric Power Systems Research*, *34*(3), 187–196.

European Environment Agency. (2019, Jun). *Heating and cooling degree days.*

Friedman, J. H. (1991). Multivariate adaptive regression splines. *The annals of statistics*, 1–67.

Gardner, M. W., & Dorling, S. (1998). Artificial neural networks (the multilayer perceptron)—a review of applications in the atmospheric sciences. *Atmospheric environment*, *32*(14-15), 2627–2636.

German Federal Foreign Office. (2020, Jun). *Germany and Luxembourg: Bilateral Relations.*

Hagan, M. T., & Menhaj, M. B. (1994). Training feedforward networks with the Marquardt algorithm. *IEEE transactions on Neural Networks*, *5*(6), 989–993.

Hinman, J., & Hickey, E. (2009). Modeling and forecasting short-term electricity load using regression analysis. *Journal of Institute for Regulatory Policy Studies*, 1–51.

Hong, T., & Fan, S. (2016). Probabilistic electric load forecasting: A tutorial review. *International Journal of Forecasting*, *32*(3), 914–938.

Hong, T., et al. (2010). Short Term Electric Load Forecasting.

Hong, T., Wilson, J., & Xie, J. (2013). Long term probabilistic load forecasting and normalization with hourly information. *IEEE Transactions on Smart Grid*, *5*(1), 456–462.

Hyndman, R. J., & Fan, S. (2009). Density forecasting for long-term peak electricity demand. *IEEE Transactions on Power Systems*, *25*(2), 1142–1153.

Jekabsons, G. (2016, May). *ARESLab: Adaptive Regression Splines toolbox.* Retrieved from `http://www.cs.rtu.lv/jekabsons/regression.html`

Karsoliya, S. (2012). Approximating number of hidden layer neurons in multiple hidden layer BPNN architecture. *International Journal of Engineering Trends and Technology*, *3*(6), 714–717.

Lusis, P., Khalilpour, K. R., Andrew, L., & Liebman, A. (2017). Short-term residential load forecasting: Impact of calendar effects and forecast granularity. *Applied Energy*, *205*, 654–669.

Magnano, L., & Boland, J. (2007). Generation of synthetic sequences of electricity demand: Application in South Australia. *Energy*, *32*(11), 2230–2243.

Marquardt, D. W. (1963). An algorithm for least-squares estimation of nonlinear parameters. *Journal of the society for Industrial and Applied Mathematics*, *11*(2), 431–441.

Metaxiotis, K., Kagiannas, A., Askounis, D., & Psarras, J. (2003). Artificial intelligence in short term electric load forecasting: a state-of-the-art survey for the researcher. *Energy conversion and Management*, *44*(9), 1525–1534.

Nalcaci, G., Özmen, A., & Weber, G. W. (2019). Long-term load forecasting: models based on MARS, ANN and LR methods. *Central European Journal of Operations Research*, *27*(4), 1033–1049.

Nelson, M., Hill, T., Remus, W., & O'Connor, M. (1999). Time series forecasting using neural networks: Should the data be deseasonalized first? *Journal of forecasting*, *18*(5), 359–367.

Palit, A. K., & Popovic, D. (2006). *Computational intelligence in time series forecasting: theory and engineering applications.* Springer Science & Business Media.

Park, D. C., El-Sharkawi, M., Marks, R., Atlas, L., & Damborg, M. (1991). Electric load forecasting using an artificial neural network. *IEEE transactions on Power Systems*, *6*(2), 442–449.

Rosenblatt, F. (1962). Principles of neurodynamics: perceptrons and the theory of brain mechanisms. *Spartan Books 7(3):1-219*.

Rumelhart, D. E., Hinton, G. E., & Williams, R. J. (1986). Learning representations by backpropagating errors. *nature*, *323*(6088), 533–536.

Zhang, G. P., & Qi, M. (2005). Neural network forecasting for seasonal and trend time series. *European journal of operational research*, *160*(2), 501–514.

10 MATLAB code

Multiple Linear Regression

```
%MODEL: Multiple Linear Regression (MLR)
%NOTE: Variables in workspace: X (explanatory) and Y (dependent) variables as well as LOAD_LU_adj (load demand).
%Author: Luc van Breukelen
x = X(1:78888,:);
y = Y(1:78888,1);

y_predict = X(78889:105192,1);
x_predict = Y(78889:105192,:);

% Simple MLR
mdl = stepwiselm(x,y,'Criterion', 'aic', 'Upper', 'linear');

% Extended MLR
mdl = stepwiselm(x,y,'Criterion', 'aic', 'Upper', 'quadratic');

% Residuals
residuals_train = table2array(mdl.Residuals);
residuals_train = residuals_train(:,1);
residuals_test =  y_predict - predict(mdl,x_predict);
```

Multivariate Adaptive Regression Splines

```
%MODEL: Multivariate Adaptive Regression Splines (MARS)
%NOTE: Variables in workspace: X (explanatory) and Y (dependent) variables as well as LOAD_LU_adj (load demand).
%
% ARESLab: Adaptive Regression Splines toolbox for Matlab/Octave
% Author: Gints Jekabsons (gints.jekabsons@rtu.lv)
% URL: http://www.cs.rtu.lv/jekabsons/
%
% Implementation written by: Luc van Breukelen.

%% Setting of paramters
maxBF = 100;
maxFinalBF = 100;
costExtraKnot = 3;
```

```
maxInteraction = 3;
params = aresparams2('maxFuncs', maxBF, 'maxFinalFuncs', ...
    maxFinalBF, 'c', costExtraKnot, 'maxInteractions', maxInteraction,...
    'cubic', false ); % piecewise-linear without minSpan

params = aresparams2('maxFuncs', maxBF, 'maxFinalFuncs', ...
    maxFinalBF, 'c', costExtraKnot, 'maxInteractions', maxInteraction,...
    'cubic', false , 'useMinSpan', 500 ); % piecewise-linear with minSpan
%% Load data
y = Y(1:78888,1);
x = X(1:78888,:);

y_predict = X(78889:105192,1);
x_predict = Y(78889:105192,:);
%% Build model
disp('Building the model =================================================');
[model, ~, resultsEval] = aresbuild(x, y, params);
%% Plotting model selection from the backward pruning phase
figure;
hold on; grid on; box on;
h(1) = plot(resultsEval.MSE, 'Color', [0 0.447 0.741]);
h(2) = plot(resultsEval.GCV, 'Color', [0.741 0 0.447]);
numBF = numel(model.coefs);
h(3) = plot([numBF numBF], get(gca, 'ylim'), '--k');
xlabel('Number of basis functions');
ylabel('MSE, GCV');
legend(h, 'MSE', 'GCV', 'Selected model');
%% Info on the basis functions
disp('Info on the basis functions =========================================');
aresinfo(model, x, y);

% Printing the model
disp('The model ===========================================================');

%% Testing on test data
disp('Testing on test data ================================================');
results = arestest(model, x_predict, y_predict);

% Residuals
```

```
residuals_train =  y-arespredict(model, x);
residuals_test =   y_predict-arespredict(model, x_predict);
```

Artificial Neural Network

```
%MODEL: Artifical Neural Network (ANN)
%NOTE: Variables needed in workspace: X and Y (explanatory & dependent variables)
    as well as LOAD_LU_adj (load demand).
%Author: Luc van Breukelen

% Data
y = Y(1:78888,1)';
x = X(1:78888,:)';

y_predict = X(78889:105192,1)';
x_predict = Y(78889:105192,:)';

% Create a Fitting Network
trainFcn = 'trainlm';
hiddenLayer1Size = 15;
hiddenLayer2Size = 15;
net = fitnet([hiddenLayer1Size, hiddenLayer2Size],trainFcn);

% Set sigmoid functions
net.layers{1}.transferFcn = 'logsig';
net.layers{2}.transferFcn = 'logsig';
net.layers{3}.transferFcn = 'purelin';
net.performFcn = 'sse';

% Set up Division of Data for Training, Validation, Testing
net.divideParam.trainRatio = 75/100;
net.divideParam.valRatio = 25/100;
net.divideParam.testRatio = 0/100;

% Train network
[net,tr] = train(net,x,y);

%Residuals
residuals_train =  y-net(x);
residuals_test =   y_predict-net(x_predict);
```

Double Seasonal Block Bootstrap

```
%Double seasonal block bootstrap method for 2015, 2016 and 2017
%NOTE: Workspace need to consist the x matrix with explanatory variables.
%Author: Luc van Breukelen

number_of_scenarios = 1000;
weather_scenarios = cell(number_of_scenarios,1);
number_variables = 7;
number_observations = 26304;
scenario = zeros(number_observations,number_variables);
default_length = 91*24;
year = 24*365;

for scenario_number = 1 : number_of_scenarios
    % First year is no leap year.
    for season = 1:4
        [start_index,end_index] = getIndex(0,season);
        scenario(1+(season-1)*default_length:(1+(season-1)*default_length)+(
            end_index-start_index),:) = x(start_index:end_index,:);
    end
    % Second year is leap year
    for season = 1:4
        [start_index,end_index] = getIndex(1,season);
        if season ==2
            scenario(year+1+(season-1)*default_length:8761+(season-1)*
                default_length+(end_index-start_index),:) = x(start_index:end_index
                ,:);
        elseif season >2
             scenario(year+1+(season-1)*default_length+24:year+1+(season-1)*
                 default_length+24 +(end_index-start_index),:) = x(start_index:
                 end_index,:);
        else
            scenario(year+1+(season-1)*default_length:year+1+(season-1)*
                default_length +(end_index-start_index),:) = x(start_index:
                end_index,:);
        end
    end
    % Third year is no leap year.
    for season = 1:4
```

```
        [start_index,end_index] = getIndex(0,season);
        scenario(year*2+24+(season-1)*default_length+1:year*2+24+(season-1)*default_length +1+ (end_index-start_index),:) = x(start_index:end_index,:);
    end
    weather_scenarios{scenario_number} = scenario; %Save scenario of 3 year.
end
```

Function for double seasonal block bootstrap

```
function [start_index,end_index] = getIndex(leap,season)
%GETINDEX Generate start and end indices of block.
%   INPUT:
%   leap        Dummy variable which is 1 when year is a leap year
%   season      Integer between [1,4] which represents number of block.
%   OUTPUT:
%   start_index Start index of block.
%   end_index   End index of block.
%Author: Luc van Breukelen

length_block = 2184;
max_index = 78888;

if (leap ==1 && season == 2) || season == 4
    length_block = length_block + 24; % Period with extra day (leap year).
end

i = 1 + floor(rand*9);  %Randomly select a year from historical dataset.

%Uniformly integer in [-14,14]
random = floor(rand * 24*28)-14*24;
random = random - mod(random,24);

start_index = max(1+(i-1)*8760+(season-1) *2184+random,1);
end_index = start_index+length_block-1;
if end_index > max_index    %Correction at end of data set.
    end_index = max_index;
    start_index = max_index-length_block+1;
end
end
```